Electroencephalographic Network Topologies Predict Antidepressant Responses in Patients With Major Depressive Disorder

Yueheng Peng, Yang Huang, *Student Member, IEEE*, Baodan Chen, Mengling He, Lin Jiang, Yuqin Li, Xunan Huang, Changfu Pei, Shu Zhang, Cunbo Li, Xiabing Zhang, Tao Zhang, Yutong Zheng, Dezhong Yao, Fali Li, and Peng Xu

***Abstract*— Medication therapy seems to be an effective treatment for major depressive disorder (MDD). However, although the efficacies of various medicines are equal or similar on average, they vary widely among individuals. Therefore, an understanding of methods for the timely evaluation of short-term therapeutic response and prediction of symptom improvement after a specific course of medication at the individual level at the initial stage of treatment is very important. In our present study, we sought to identify a neurobiological signature of the response to short-term antidepressant treatment. Related brain network analysis was applied in resting-state electroencephalogram (EEG) datasets from patients with MDD. The corresponding EEG networks were constructed accordingly and then quantitatively measured to predict the efficacy after eight weeks of medication, as well as to distinguish the therapeutic responders from non-responders. The results of our present study revealed that the corresponding resting-state EEG networks became significantly weaker after one week of treatment, and the eventual medication efficacy was reliably predicted using the changes in those network properties within the one-week medication regimen. Moreover, the corresponding resting-state networks at baseline were also proven to precisely distinguish those responders from other individuals with an accuracy of 96.67% when using the spatial network topologies as the discriminative features. These findings consistently provide a deeper neurobiological understanding of antidepressant treatment and a reliable and quantitative approach for personalized treatment of MDD.**

***Index Terms*— Major depressive disorder, resting-state EEG, clinical therapy, prediction.**

Manuscript received 12 January 2022; revised 6 May 2022 and 5 August 2022; accepted 28 August 2022. Date of publication 31 August 2022; date of current version 15 September 2022. This work was supported in part by the National Natural Science Foundation of China under Grant U19A2082, Grant 61961160705, Grant 62103085, and Grant 8210217; in part by the Project of Science and Technology Department of Sichuan Province under Grant 2021YFSY0040 and Grant 2020ZYD013; and in part by the Science and Technology Development Fund, Macau, SAR, under Grant 0045/2019/AFJ. *(Corresponding authors: Fali Li; Peng Xu.)*

This work involved human subjects or animals in its research. The authors confirm that all human/animal subject research procedures and protocols are exempt from review board approval.

Yueheng Peng, Baodan Chen, Mengling He, Lin Jiang, Yuqin Li, Changfu Pei, Shu Zhang, Cunbo Li, Xiabing Zhang, Tao Zhang, and Yutong Zheng are with the MOE Key Laboratory for Neuroinformation, Clinical Hospital of Chengdu Brain Science Institute, University of Electronic Science and Technology of China, Chengdu 611731, China, and also with the School of Life Science and Technology, Center for Information in Medicine, University of Electronic Science and Technology of China, Chengdu 611731, China.

Yang Huang is with the Department of Electrical Engineering and Computer Science, University of Tennessee Knoxville, Knoxville, TN 37996 USA.

Xunan Huang is with the MOE Key Laboratory for Neuroinformation, Clinical Hospital of Chengdu Brain Science Institute, University of Electronic Science and Technology of China, Chengdu 611731, China, also with the School of Life Science and Technology, Center for Information in Medicine, University of Electronic Science and Technology of China, Chengdu 611731, China, and also with the School of Foreign Languages, University of Electronic Science and Technology of China, Chengdu 611731, China.

Dezhong Yao is with the MOE Key Laboratory for Neuroinformation, Clinical Hospital of Chengdu Brain Science Institute, University of Electronic Science and Technology of China, Chengdu 611731, China, also with the School of Life Science and Technology, Center for Information in Medicine, University of Electronic Science and Technology of China, Chengdu 611731, China, also with the School of Electrical Engineering, Zhengzhou University, Zhengzhou 450001, China, and also with the Research Unit of Neuroinformation (2019RU035), Chinese Academy of Medical Sciences, Chengdu 610072, China.

Fali Li and Peng Xu are with the MOE Key Laboratory for Neuroinformation, Clinical Hospital of Chengdu Brain Science Institute, University of Electronic Science and Technology of China, Chengdu 611731, China, also with the School of Life Science and Technology, Center for Information in Medicine, University of Electronic Science and Technology of China, Chengdu 611731, China, and also with the Research Unit of Neuroinformation (2019RU035), Chinese Academy of Medical Sciences, Chengdu 610072, China (e-mail: fali.li@uestc.edu.cn; xupeng@uestc.edu.cn).

Digital Object Identifier 10.1109/TNSRE.2022.3203073

I. Introduction

MAJOR depressive disorder (MDD) is a severe mental disorder characterized by sustained negative mood [1], a persistent lack of motivation, and difficulty experiencing pleasure that substantially affects patients' quality of daily life [2]. Overall, 78% of patients with severe depression were diagnosed with at least one comorbid psychiatric disorder, such as psychotic disorder, past panic disorder, anxiety, and even suicide risk [3], [4]. MDD is not a homogeneous disorder but a complex disease with a variety of etiologies. Many studies have also shown dysfunctions in the areas of the brain modulated by corresponding systems, including the frontal cortex, amygdala, hippocampus, and basal ganglia, in depression patients. These specific brain regions are highly vulnerable to the effects of stress, probably accounting for the adverse effects of life events on MDD [5]. The severity of MDD is indexed by a composite of several behavioral measures or aspects of depressive perception. Therefore, clinicians score the degree of depressive symptoms using the 17-item clinician-administered

This work is licensed under a Creative Commons Attribution 4.0 License. For more information, see https://creativecommons.org/licenses/by/4.0/

Hamilton Depression Rating Scale ($HAMD_{17}$), which classifies patients with MDD into 4 grades on a 54-point scale using a 17-item questionnaire ranging from normal (0-7 points), mild depression (8-16 points), and moderate depression (17-23 points) to severe depression (> 24 points) [6].

Multiple therapies have been proposed and verified to be available and effective for MDD, among which psychotherapy and medications have been widely used [7]. For patients suffering from dysthymia, medication is more effective than psychotherapy, whereas blended treatment does not result in greater efficacy than either medication or psychotherapy [8]. Sertraline and escitalopram are often considered the first-line medicines for the treatment of depression [9]. Although different antidepressants display similar efficacy on average [10], the treatment selection is not effective for all patients with MDD [11]. Since the efficacy of different medicines is highly divergent, patients who exhibit a poor response to one treatment, up to one-half, attain a benefit after changing to another medicine [12]. Unfortunately, more than half of patients do not complete follow-up visits, leading them to fail to receive additional medication options [13]. Even for patients who return to pursue further treatment and finally benefit from second-line medicines, failing to obtain effective therapy at the initial stage of treatment substantially extends their treatment period (the time lag is up to 6 weeks), imposing a substantial burden on them [14]. Therefore, accurately matching patients with the best initial treatment might provide tremendous advantages to people suffering from MDD.

Recently, researchers have tried to identify biomarkers that will inform the choice of specific medications [8], [15]. For example, Wu and colleagues designed a latent-space machine-learning algorithm that utilized band power as the feature to predict symptom improvement in a manner specific to the antidepressant sertraline [16]. This approach, however, is unable to show the overall relationship among related brain regions. Band power did not work effectively in distinguishing non-responders from responders at baseline. In essence, in addition to the local band power, the global interregional couplings in the brain measured using electroencephalogram (EEG) have been reported to be a more objective measure for quantitatively evaluating therapeutic efficacy [17], [18]. In fact, analyzing the inherent information recorded by EEG provides the opportunity to investigate the network architecture of the brain, revealing the information propagation and exchange among different regions [19], [20], [21], [22]. Specifically, the corresponding information is usually processed among those spatially distributed but functionally interacting brain areas [22], [23], [24], which maps the spatial topological architecture that illustrates the neurophysiological pathogenicity of MDD [2], [25]. As reported previously, Shim and colleagues obtained a broader view of the brain with longer path length and decreased clustering coefficient in alpha and theta bands, which illustrated the deficient connectivity in patients with depression [26]. In another study, Li and colleagues reported abnormally increased synchronization consisting of denser short-range frontal and temporal-parietal connections for an n-back task, explaining the compensatory mechanism for memory impairment in patients with depression [27].

Furthermore, investigators have recently utilized related brain networks to distinguish the differences between patients with MDD and healthy controls, assisting in providing a better understanding of the mechanism underlying depression [28], [29]. For example, in a previous study conducted by Mohammadi and Moradi, the potential relationship between the regional activity in patients with MDD and their depression severity was not only identified but also provided a quantitative depression severity prediction [30]. Gamma wave coherence has also been found to help discriminate patients with mild depression from healthy controls, as they manifested lower gamma coherence than healthy controls [31]. However, studies of the treatment response, especially short-term treatment response, thus far, are not yet sufficient and still await further investigation by performing EEG network analyses. Consequently, the identification of robust predictors provides significant benefits in terms of understanding and predicting that variation [15].

In the present study, the data we utilized were downloaded from a public data archive, the National Institute of Mental Health Data Archive (NDA). The data are publicly available through the official website (https://nda.nih.gov/edit_collection.html?id=2199). Recently, multiple studies have been conducted using these datasets. For example, Zhang and colleagues identified clinically relevant MDD subtypes using (un)supervised machine learning based on distinct network patterns [1]. Yu and colleagues investigated network differences within and between resting-state networks in patients with MDD and healthy controls and found that traumatic childhood experiences and dimensional symptoms are linked to abnormal network architecture in these patients with MDD [32]. Although these studies have been implemented, the treatment response, especially short-term treatment response, has not yet been studied extensively and is still awaiting further investigation by performing EEG network analyses. Therefore, in our present study, we analyzed the resting-state EEG datasets from patients with MDD collected before and after their one-week antidepressant medication therapy. Related brain networks of these patients with MDD were constructed and then statistically compared to explore the brain fluctuations after one-week medication, as well as predict its eight-week efficacy.

II. Materials And Methods

A. EEG Data

The EEG data were selected from the study "Establishing Moderators and Biosignatures of Antidepressant Response in Clinic Care (EMBARC)" in the National Institute of Mental Health Data Archive (NDA). In this study, patients were recruited from different centers. However, in addition to Columbia University, data from fewer qualified subjects were obtained from the other centers due to the poor quality of EEG data and failure of follow-up visits in the later stage of medication therapy. Therefore, only the EEG data from 30 patients treated at Columbia University were included in our current study. The 30 participants with MDD participated in a randomized trial and received sertraline, and their clinical and biological markers of outcomes were evaluated [33]. In detail,

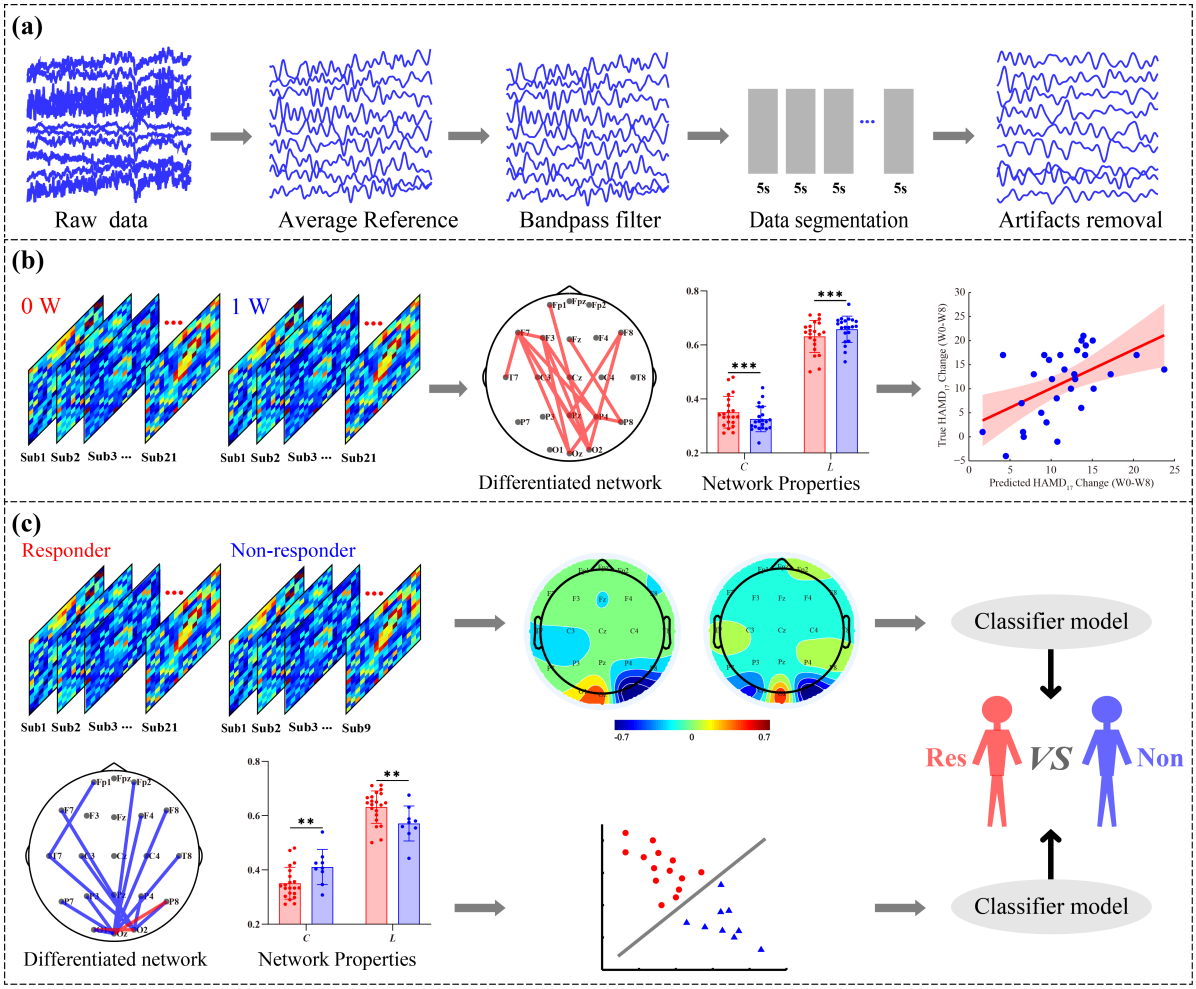

Fig. 1. Procedures used to analyze resting-state EEG datasets. (a) Preprocessing of the resting-state EEG datasets, (b) Prediction of the treatment outcome based on resting-state EEG networks, and (c) Discrimination of responders and non-responders based on resting-state EEG networks.

the 30 subjects were assigned to an 8-week treatment of sertraline of up to 200 mg daily. Sertraline dose adjustments occurred at weeks 1, 2, 3, 4, 6, and 8 to ensure delivery of the appropriate dose and to record the symptom reduction (measured by $HAMD_{17}$). The raw data for each patient included two 2-min blocks of eyes-opened resting EEG. The EEG datasets were collected at Columbia University/Stony Brook (Data Center) in the United States at baseline (0 W) and one week after the treatment (1 W) using a high-density EEG system (BioSemi, 72 channels). During online data recording, patients were seated in a quiet and electrically shielded room with their eyes open and relaxed as much as possible, and electrodes PPO1 and PPO2 served as the reference. EEG signals were sampled at 256 Hz and online bandpass filtered at 0-251.3 Hz. At week 8, the 30 patients were assessed with the Clinical Global Improvement scale (CGI), and subjects who received a CGI score worse than "much improved" (i.e., having a CGI score greater than 2) were deemed non-responders, while the remaining patients who scored "much improved" or "very much improved" (i.e., having a CGI score of 1 or 2) were considered responders.

B. Methods

In this study, resting-state EEG datasets were used to construct the corresponding brain networks with MATLAB v2014a software (The MathWorks Inc.). The data analysis procedure is presented in Fig. 1. Detailed descriptions of data processing are provided in the subsequent sections.

1) EEG Preprocessing: In the present study, we mainly focused on investigating the potential capacity of the resting-state brain network to quantitatively evaluate the brain fluctuations after short-term medication and distinguish responders from non-responders. Therefore, concerning these resting-state EEG datasets, before preprocessing, the first and last ten seconds of EEG signals were first excluded, and multiple preprocessing procedures were then applied to complete data preprocessing, which included averaging-referencing, [1], [42] Hz bandpass filtering, and 5-s-length data segmentation. Thereafter, a threshold of $\pm 100\ \mu V$ was subsequently used to automatically exclude segments with absolute magnitudes exceeding 100 μV from any recorded electrode. Additionally, as denser electrodes might provoke more severe volume conduction effects on connectivity, sparse electrodes were used to reduce the effect of volume conduction on EEG networks. Concretely, 21 of 72 channels, according to the international 10-20 system, were selected in our present study to perform the analyses described below.

2) Functional Brain Networks: As proven in previous studies, brain network analysis is remarkably helpful in explaining the neurophysiological pathogenicity of MDD [2], and a related analysis was thus implemented in our study. Actually,

an EEG network has been typically modeled as a collection of nodes (i.e., EEG electrodes) and edges that are evaluated between paired electrodes [34], [35]. When constructing the corresponding EEG network for all patients with MDD, the same definition of the EEG network is considered. Specifically, we set 21 electrodes as the network nodes, and after extracting the EEG signal for each electrode, the estimated paired-electrode interactions were then regarded as the network edges. Here, when constructing resting-state networks for patients with MDD, the synchronization likelihood between pairwise electrodes was considered [36], [37]. As suggested in previous studies, the phase locking value (PLV) [38], [39] that experts in estimating the phase synchronization among pairwise signals was thus adopted, leading to an adjacency matrix with the dimension of electrodes $\times$ electrodes. Within the PLV network, the PLV value is defined within the range of [0, 1], and higher PLV values represent a stronger strength of phase synchronization.

As formulated, the Hilbert transform (HT) is used to form the analytical signal $H(t)$ and estimate the corresponding instantaneous phases $\varphi_x(t)$ and $\varphi_y(t)$ of two given time series $x(t)$ and $y(t)$ as follows:

$$\begin{cases} H_x(t) = x(t) + i\,HT_x(t) \\ \mathrm{H}_y(t) = y(t) + i\,HT_y(t) \end{cases} \tag{1}$$

where $HT_x(t)$ and $HT_y(t)$ are the HTs of both time series, $x(t)$ and $y(t)$, which are defined as follows:

$$\begin{cases} HT_x(t) = \dfrac{1}{\pi} P.V. \displaystyle\int_{-\infty}^{\infty} \frac{x(t')}{t - t'} dt' \\ HT_y(t) = \dfrac{1}{\pi} P.V. \displaystyle\int_{-\infty}^{\infty} \frac{y(t')}{t - t'} dt' \end{cases} \tag{2}$$

where the *P.V.* denotes the Cauchy principal value. Afterward, the corresponding analytical signal phases, i.e., $\varphi_x(t)$ and $\varphi_y(t)$, were computed as follows:

$$\begin{cases} \varphi_{\mathrm{x}}(t) = \arctan \dfrac{HT_x(t)}{x(t)} \\ \varphi_{\mathrm{y}}(t) = \arctan \dfrac{HT_y(t)}{y(t)} \end{cases} \tag{3}$$

Finally, the PLV was formulated as follows:

$$\mathrm{w}^{plv} = \left| \frac{1}{N} \sum_{j=0}^{N-1} e^{\mathrm{i}(\varphi_x(j\Delta t) - \varphi_y(j\Delta t))} \right| \tag{4}$$

where w^{plv} is the connection weight estimated using the PLV, Δt is the sampling period, and N denotes the sample number.

Concretely, based on those artifact-free resting-state EEG segments from each patient, the PLV was first applied to each segment to acquire the corresponding 21 $\times$ 21 adjacency matrix. For each patient with MDD, the final weighted resting-state brain network was obtained by averaging matrices across all artifact-free resting-state segments. Thereafter, based on these EEG networks, either paired or independent t-tests were used to elucidate potential differences in brain architectures between baseline (0 W) and one week after the treatment (1 W) or between responders and non-responders, respectively.

Furthermore, two weighted network properties were calculated using these constructed EEG networks, the clustering coefficient (C) and characteristic path length (L), to quantitatively measure the network efficiency in processing information. Here, these properties were calculated from the weighted EEG networks without any thresholding processing. Concretely, d_{ij} represents the shortest weighted path length between nodes i and j, n represents the number of network nodes, and Ψ represents the total set of network nodes. The two parameters were formulated as follows:

$$C = \frac{1}{n} \sum_{i \in \Psi} \frac{\sum_{j,h \in \Psi} \left(w_{ij}^{plv} w_{ih}^{plv} w_{jh}^{plv} \right)^{1/3}}{\sum_{j \in \Psi} w_{ij}^{plv} \left(\sum_{j \in \Psi} w_{ij}^{plv} - 1 \right)} \tag{5}$$

$$L = \frac{1}{n} \sum_{i \in \Psi} \frac{\sum_{j \in \Psi, j \neq i} d_{ij}}{n - 1} \tag{6}$$

Afterward, we statistically analyzed the potential differences in these weighted network properties between responders and non-responders using an independent t-test and between 0 W and 1 W using a paired t-test, which was then corrected for multiple tests using the Bonferroni correction to further validate treatment response in patients with MDD.

3) The Prediction of Medication Efficacy Using a Multiple Linear Regression Model: In the present study, the changes in the two resting-state network properties (i.e., ΔC and ΔL) were selected as the variables in the multiple linear regression model for building a model to predict medication efficacy. Based on both ΔC and ΔL, the corresponding prediction model was formulated as follows:

$$\mathrm{Y} = \beta_0 + \beta_1 \Delta \mathrm{C} + \beta_2 \Delta \mathrm{L} + \varepsilon \tag{7}$$

where Y denotes the predicted eight-week medication efficacy, $\beta_{0\ldots2}$ denotes the regression coefficients of the network property changes, and ε denotes the error term.

Here, the leave-one-out cross-validation (LOOCV) strategy was used to predict the eight-week medication efficacy in all patients with MDD [40]. Specifically, for N samples (N = 30 in this study), N-1 samples were used for training, and the remaining 1 sample was used for testing in each LOOCV run. The regression coefficient for each variable was estimated to build a prediction model for the current N-1 samples, which was then used to predict the treatment outcome of an individual in the test set. This procedure was repeated N times until all samples served as testing sets one time.

4) Discrimination of Responders From Non-Responders Based on Resting-State Networks: Eventually, these resting-state networks were further tested to prove whether they also promote the clinical selection of optimal therapeutic strategies for MDD, which were validated using two different types of network features. First, these resting-state network properties were adopted. In detail, all of these patients with MDD were divided into training and testing subgroups. During the training process, the corresponding training weighted network properties (i.e., C and L) were calculated using Eqs. (5) and (6). Second, the linear discriminant

analysis (LDA) classifier was trained on these training features. Thereafter, during the testing process, those testing network properties were also calculated accordingly and then input into the trained LDA classifier, which finally discriminated the testing data into responders or non-responders, and output the classification accuracy.

As proven previously, these network properties are direct statistical measurements of brain networks. Although they might also quantitatively capture the overall network differences under our conditions of interest, the corresponding spatial network information is still unmined [41]. Thus, the network property can be used to describe the overall brain network but does not encompass all features contained in the network topology. In our previous studies, we developed the spatial pattern of the network (SPN) [42] to extract the discriminative spatial pattern contained in a given brain network [42]. As the SPN was described in detail in our previous studies [42], a brief introduction to this method was primarily provided here.

M_1 and M_2 correspond to the adjacency matrices for responders and non-responders estimated using PLV, respectively. The SPN filters are the projections derived by maximizing the following function:

$$J(z) = \frac{zM_1M_1^Tz^T}{zM_2M_2^Tz^T} = \frac{z\mathrm{A}_1z^T}{z\mathrm{A}_2z^T} \tag{8}$$

where z denotes the SPN filter (an objective projection) and A_1 and A_2 are the covariance matrices of the adjacency matrices M_1 and M_2, respectively.

Because the scaling of projection z will have no effect on the object value, Eq. (8) can be rewritten as the following constrained optimization problem:

$$\begin{cases} arg\max\limits_{z} & z\mathrm{A}_1\mathrm{z}^{\mathrm{T}} \\ subject\ to & z\mathrm{A}_2\mathrm{z}^{\mathrm{T}} = 1 \end{cases} \tag{9}$$

By introducing the Lagrange multiplier, Eq. (9) can be further rewritten as follows:

$$\mathrm{L}(z, \lambda) = z\mathrm{A}_1z^T - \lambda(z\mathrm{A}_2z^T - 1) \tag{10}$$

Then, the objective projection z is estimated utilizing the generalized eigenvalue equation by taking the derivative of Eq. (10) with respect to z under the condition $\frac{\partial L}{\partial z} = 0$,

$$\mathrm{A}_1\mathrm{z}^{\mathrm{T}} = \lambda\mathrm{A}_2z^T \tag{11}$$

where λ denotes the eigenvalue of the generalized eigenvalue equation, and z is the corresponding eigenvector.

For multiple i SPN filters, Eq. (11) is solved as follows:

$$\mathrm{A}_2^{-1}\mathrm{A}_1Z^T = \sum Z^T \tag{12}$$

where Z is composed of the eigenvectors of A-1 $2\mathrm{A}_1$ and $\sum =$ diag (λ_1, λ_2, …, λ_i) with λ representing the corresponding singular values.

Additionally, given the adjacency matrices of the depression patients, the corresponding SPN features (F_{SPN}) were calculated using the following equation:

$$\begin{aligned} F_{SPN} &= log(var(V_{SPN}^TM)) \\ withV_{SPN} &= [z_1, z_2, \ldots, z_i] \end{aligned} \tag{13}$$

where M denotes the adjacency matrix of patients with MDD, z denotes the SPN filter (an objective projection), and V_{SPN} is a $21 \times i$ matrix composed of SPN filters.

As clarified in previous studies, the increasing pairs of SPN filters might facilitate the classification of situations of interest [41], [42]; for example, different pairs of SPN features (i.e., 1 pair, 2 pairs, and 3 pairs) have been used to achieve the classification of psychogenic nonepileptic seizures from epilepsy, and 3 pairs of SPN features achieved the highest classification accuracy [42]. Consistent with the protocols used in previous studies [43], [44], in our present study, three pairs of SPN filters were accordingly adopted to achieve the classification of responders and non-responders. In particular, for a 21×21 adjacency matrix, M, each SPN filter was a 21-length vector, and therefore, three pairs of SPN filters comprised a 21×6 matrix. Afterward, the corresponding SPN features were acquired as a vector with a length of 6 by applying these SPN filters to the constructed resting-state EEG networks and then calculating the variance of each row of weighted nodes.

When using the SPN features to classify the responders and non-responders, protocols similar to those used to analyze network properties were performed. Specifically, after acquiring the trained SPN filters during the training process, we subsequently calculated the corresponding training SPN features (Eq. (13)) that would be used to train the LDA classifier. Additionally, the trained filters were further applied to the testing sets to acquire the testing SPN features. Eventually, the testing SPN features were input into the trained LDA classifier, and the related classification performance was evaluated accordingly.

As the present dataset was relatively small, the LOOCV test was also used to recognize responders and non-responders, as described in previous studies [45], [46]. Based on the LOOCV, the corresponding indices, including accuracy (*ACC*), sensitivity (*SEN*), and specificity (*SPE*), were then calculated to evaluate the performance. Let N_{Res} and N_{Non} denote the total number of responders and non-responders, respectively, and let n_{Res} and n_{Non} denote the correctly discriminated number of responders and non-responders, respectively. The detailed equations used to calculate these indices were as follows:

$$ACC = \frac{n_{Res} + n_{Non}}{N_{Res} + N_{Non}} \times 100\% \tag{14}$$

$$SEN_{Res} = \frac{n_{Res}}{N_{Res}} \times 100\% \tag{15}$$

$$SPE_{Non} = \frac{n_{Non}}{N_{Non}} \times 100\% \tag{16}$$

III. Results

A. Comparison of $HAMD_{17}$ Scores Between Responders and Non-Responders at Baseline and After One Week of Medication

Medication treatment visits occurred at baseline and weeks 1, 2, 3, 4, 6, and 8 to ensure that the delivery was appropriate and to record the HAMD_{17}score. Although these scales have some defects, they are still currently crucial for the

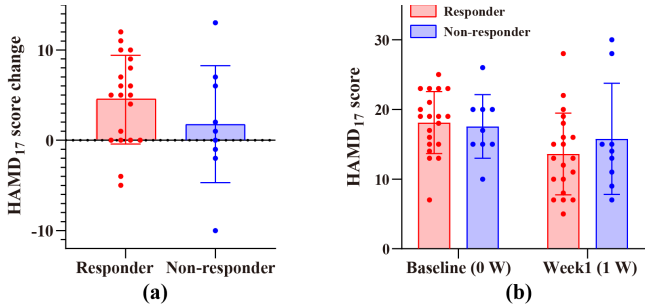

Fig. 2. Statistical differences in $HAMD_{17}$ scores between non-responders and responders. (a) $HAMD_{17}$ score fluctuations after one week of antidepressant medication. (b) $HAMD_{17}$ scores at baseline and week 1.

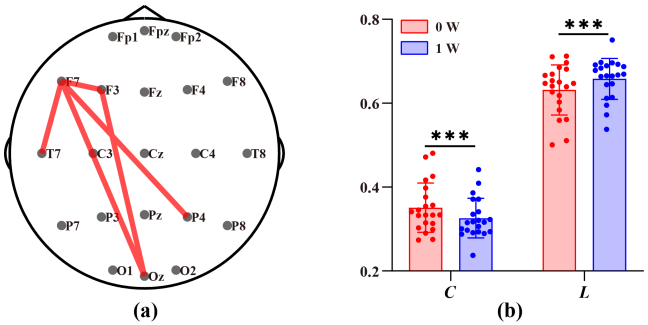

Fig. 3. The significant differences in network topology and properties in responders between 0 W and 1 W. (a) Network topology. (b) Network properties.

clinical diagnosis of related diseases, and the classification in the neuroscience field also uses clinical scales as the evaluation criteria [47], [48]. Therefore, using the same protocol described in previous studies [49], [50], these clinical scores of all patients were also recorded as the "gold standard" when evaluating and classifying the patients. Concretely, considering the EEG datasets used in this study and methods reported in previous studies [51], [52], 30 patients were assessed with the CGI at the 8th week. In addition, expanding on the CGI criteria, 9 patients who received a score worse than "much improved" were deemed to be medication non-responders, while the remaining 21 patients who scored "much improved" or "very much improved" were then considered responders [33]. The 0 W minus 1 W fluctuations in $HAMD_{17}$ scores were primarily calculated to quantify the efficacy of the antidepressant medication; unfortunately, as displayed in Fig. 2(a), no statistically significant differences were identified in $HAMD_{17}$ score fluctuations for both patient groups. Because resting-state EEG datasets were only collected at two stages, i.e., at baseline and week 1, the efficacy within the relatively short medication duration (i.e., only baseline and week 1) was also considered. Concretely, the corresponding differences in $HAMD_{17}$ scores between the responders and non-responders were statistically analyzed at both baseline and week 1. Not surprisingly, no significant differences in $HAMD_{17}$ scores were observed between the two groups at either stage ($p > 0.05$), as shown in Fig. 2(b).

B. Brain Fluctuations After Short-Term Medication Indexed by Resting-State EEG Networks

1) Network Differences Between 0 W and 1 W: Next, we sought to identify a robust biomarker that quantitatively evaluated patients' brain fluctuations after one-week antidepressant treatment, which might help predict the final medication efficacy in patients with MDD. Here, expanding upon the constructed resting-state EEG networks for all patients, the corresponding implicit spatial network topologies and related network properties, were first statistically compared to validate the sensitivity of network measures to antidepressant treatment.

On the one hand, we concentrated on the corresponding network topologies measured for responders in both stages. Fig. 3(a) shows the significant differences in network topologies between baseline (i.e., 0 W) and one week of medication (i.e., 1 W), in which the red solid lines denote the reduced interelectrode connectivity (0 W > 1 W). Specifically, relatively stronger connectivity (i.e., red long-range edges) among the frontal and occipital lobes was observed at the baseline stage ($p < 0.05$, Bonferroni-corrected) than at 1 W. Thereafter, the network properties, including C and L, were calculated and compared to quantitatively measure the network fluctuation after one week of treatment, as shown in Fig. 3(b), in which the red and blue bars denote the network properties corresponding to 0 W and 1 W, respectively. Herein, to statistically explore the potential differences, the linear mixed model was adopted. In detail, the model included the network properties (e.g., clustering coefficients) as the dependent variable, Time (0 W and 1 W) and Group (responder and non-responder) were then treated as independent variables. In addition, the model included participants as the random factor. Models were then compared using log-likelihood ratio tests to determine the best model, and backward algorithms were used for model comparisons. The results showed that the best-fit model included the main effect of Group and Group-x-Time interactions. Herein, when taking the network properties of Week 0 and the non-responders as the baselines, the statistics demonstrated that for responders, C showed a decreasing trend at 1 W compared to 0 W, while L showed an increasing trend. Although the non-responders received one week of antidepressant medication treatment, significant differences ($p > 0.05$) were not observed either in network topology or in properties between the two stages.

2) Prediction of the Medication Efficacy Based on Resting-State Network Properties: Because these resting-state network characteristics (both topologies and properties) were identified to help evaluate the brain fluctuations after one-week medication therapy, we then intended to explore whether any potential relationship between the $HAMD_{17}$ score fluctuations and the corresponding network property changes (ΔC and ΔL) would be identified. As shown in Fig. 4, within the alpha band, ΔC ($r = 0.426$, $p = 0.019$) showed a significant positive correlation with the change in the $HAMD_{17}$ score at one week, while ΔL was negatively correlated with the change in the $HAMD_{17}$ score ($r = -0.428$, $p = 0.018$). In fact, these patterns were also observed within multiple bands, e.g., delta, theta, and beta bands. As similar findings across multiple bands were acquired and the activity of the alpha band in the brain at rest

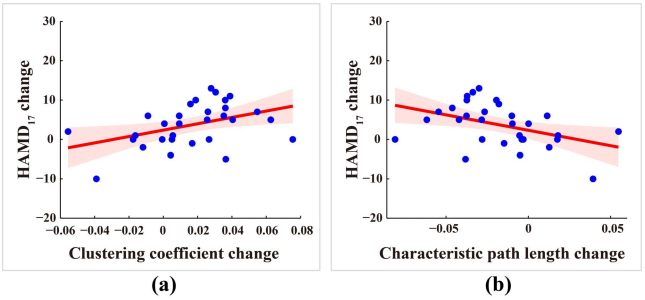

Fig. 4. Relationships between changes in the network properties and changes in the $HAMD_{17}$ score during one week of medication. In each subfigure, the red line is the fitted curve, and the blue filled circles denote the patients with MDD.

has been proven to be a capable discriminator [2], as well as the page limitation, further analyses, such as correlations and predictions, were only reported for the alpha band in the present study.

In addition to the potential relationship between network property changes and changes in the $HAMD_{17}$ score at one week, related network properties were analyzed to clarify whether they might also facilitate the prediction of treatment outcomes; in particular, we predicted the treatment efficacy after eight weeks of medication. Here, the eventual treatment efficacy was quantified as the difference in $HAMD_{17}$ scores at baseline from the 8th week, and the differences in network properties between the baseline and one-week medication were used as the corresponding predicting features. By implementing the linear prediction analysis, we then predicted the changes in the $HAMD_{17}$ score for all patients with MDD. Consequently, as displayed in Fig. 5, the predicted changes in $HAMD_{17}$ scores were significantly related to the actual changes. The corresponding Pearson's correlation coefficient was $r = 0.53$ ($p = 0.002$), and the Root Mean Squared Error (RMSE) was 5.973. Here, we randomly scrambled the network properties and $HAMD_{17}$ scores of all patients and then repeated the prediction 1000 times to further clarify that the current prediction result was not achieved by chance using the protocols described in previous studies [53]. Subsequently, by statistically investigating these permutation results, we found that a correlation coefficient of 0.53 reached a significance level of 0.001.

C. Medication Sensitivity of Patients With MDD Derived From Resting-State Networks

1) Network Differences Between Responders and Non-Responders: The differences in resting-state EEG networks between responders and non-responders were also investigated at the baseline and one-week medication stages to further validate the great potential of network characteristics in determining the response of medication therapy in patients with MDD. Fig. 6(a) and (b) illustrate the significant differences in network topology and properties between the two groups. Concretely, Fig. 6(a) displays the topological difference at baseline, in which weaker linkages are identified for the responders than for the non-responders. In addition, the corresponding differences ($p < 0.05$) in network properties further

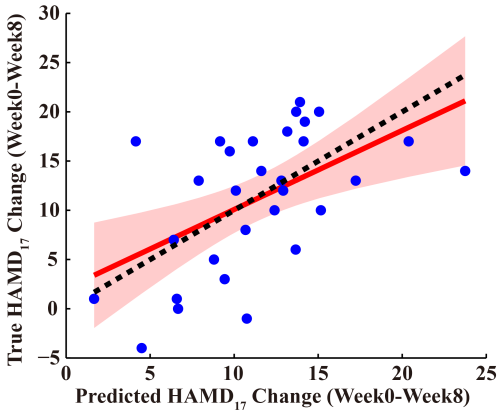

Fig. 5. Prediction of eight-week medication efficacy (changes in the $HAMD_{17}$ scores) based on the resting-state network properties. The black dashed line indicates the ideal prediction, the red line fits the scatter points, and the blue filled circles denote the subjects.

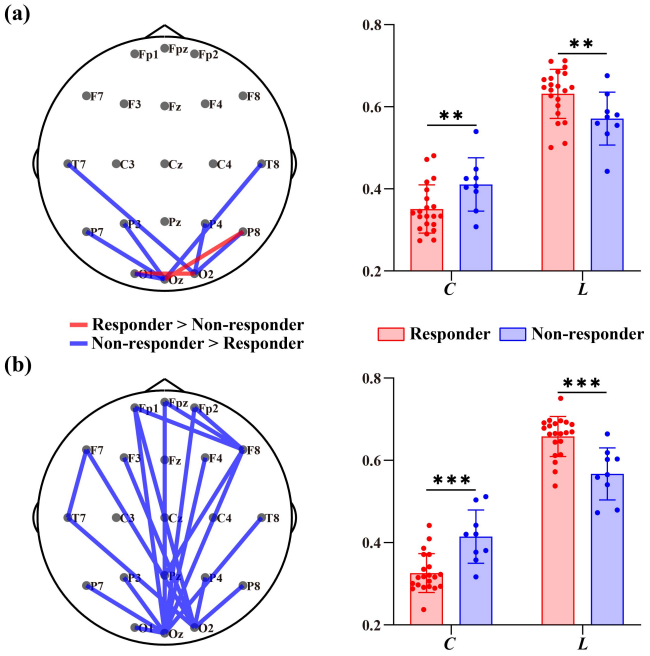

Fig. 6. The significant differences in network topology and properties between responders and non-responders at 0 W and 1 W: (a) 0 W and (b) 1 W.

clarified the smaller C and longer L for responders. At the one-week medication stage, the potential differences ($p < 0.05$) in both network topology and properties between the responders and non-responders were further increased.

2) Categorization Into Responders and Non-Responders Based on Resting-State Networks: Based on the statistically significant difference in network properties between responders and non-responders at the baseline stage shown in Fig. 6(a), we next examined whether the corresponding network properties also discriminated non-responders from responders before the actual treatment, which might facilitate the precise treatment of MDD in the clinic if this medication therapy was effective in these patients with MDD. These results might guide the design of a more effective treatment protocol. In fact, although significant differences in network properties were identified between both groups, the 76.67% classification accuracy acquired here was not as satisfying as

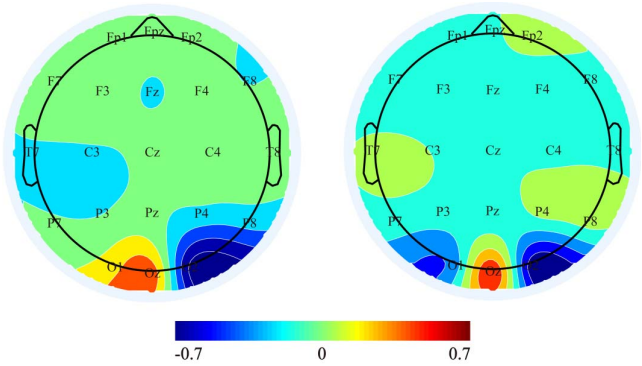

Fig. 7. Topological distribution of the most discriminative first pair of SPN filters between responders and non-responders. The subfigures in the left and right columns denote the corresponding spatial Filters 1 and 2, respectively.

expected, as well as the sensitivity of 76.19% for responders and the specificity of 77.78% for non-responders.

In addition to the network properties, which mainly serve as the direct statistical measures of brain networks, the corresponding spatial network topologies [41] had been fully proven to facilitate our classification analysis. Therefore, based on our developed SPN method, related implicit and inherent spatial network features (i.e., SPN features) were first extracted from the resting-state EEG data from both responders and non-responders at 0 W and further utilized to classify both groups.

Here, we primarily showed the most discriminative pair of SPN filters (i.e., Filters 1 and 2), as shown in Fig. 7, in which those network nodes (e.g., electrodes O1, O2, and Oz) that exhibited significant edge differences in Fig. 6(a) displayed with larger coefficients (i.e., marked with deep red or blue color). We then used these SPN features as the discriminative features to classify responders and non-responders. Here, the LOOCV strategy was utilized to complete the categorization, and as expected, an improved performance (i.e., an accuracy of 96.67%) was indeed acquired, along with a sensitivity of 100% for responders and a specificity of 88.89% for non-responders.

D. Categorization of Merged Responders and Non-Responders From Different Sites

Considering the EMBARC recorded EEG datasets from four different sites, after testing on the participants of Columbia University, participants of the other three sites were reviewed following the same strategy used at Columbia University. Even though the EEG datasets had fewer qualified patients, both responders and non-responders could be still identified. Eventually, a total of 80 participants were picked and then included in the further categorization analysis. Just as displayed in Fig. 8, we extracted the scatter diagram of the corresponding SPN features from the first pair of filters with the most distinguishing power. From this scatter diagram, we can see that the responders and non-responder can be well distinguished; and the recognition of responders from non-responders also obtained acceptable performance, as the accuracy of 77.50% was achieved when using SPN features as the discriminative features.

And based on these merged participants, the prediction was also achieved. Herein, by further using related network

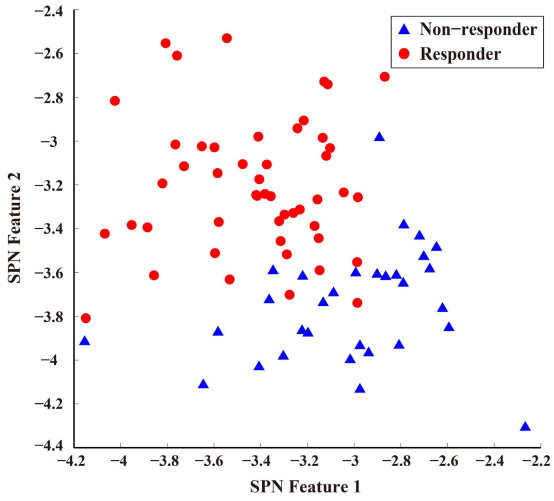

Fig. 8. Classification of responders and non-responders based on related network topologies. The scatterplot corresponding to the SPN features extracted from the first pair of the most discriminating filters between the Responders and Non-responders.

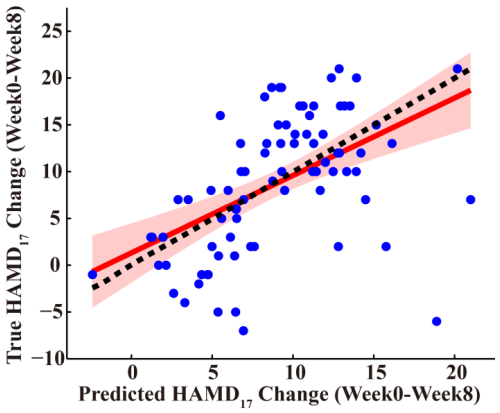

Fig. 9. Prediction of eight-week medication efficacy for site-merged participants. The black dashed line indicates the ideal prediction, the red-solid line fits the scatter points, and the blue-filled circles denote the site-merged participants.

metrics to predict the efficacy after eight-week medication, as displayed in Fig. 9, the predicted $HAMD_{17}$ changes were indeed correlated with diagnosed ones ($r = 0.50$, $p = 0.001$, $RMSE = 6.31$).

IV. Discussion

The $HAMD_{17}$ is the most widely used clinician-administered depression assessment scale, containing 17 items assessing depression experienced over previous weeks, which provides an indication of depression and serves as a guide to evaluate recovery. Considering the reliability and validity of $HAMD_{17}$ [54], we analyzed $HAMD_{17}$ scores recorded in the first two stages to illustrate the treatment efficacy after a relatively short-term medication period, as well as to explore if the $HAMD_{17}$ was highly sensitive in identifying responders and non-responders. Concretely, we sought to use the efficacy of one week of medication to classify these patients with MDD. As illustrated in our present study, although these patients were divided into responders and non-responders based on their eventual $HAMD_{17}$ scores recorded after eight weeks of medication, no significant difference was observed when we

first explored the potential fluctuations in $HAMD_{17}$ scores between 0 W and 1 W of medication. Therefore, the model failed to describe the one-week treatment efficacy and further discriminate responders and non-responders. As changes in the $HAMD_{17}$ score did not show an obvious difference in distinguishing responders from non-responders, the $HAMD_{17}$ scores were then directly compared between responders and non-responders at the two time points mentioned above. Unfortunately, the responders did not show a significant difference from the non-responders at either stage, as shown in Fig. 2(b). These results might be attributed to the fact that the short-term treatment was not long enough to significantly affect the brain of patients with MDD and failed to alter the $HAMD_{17}$ score [55]. Clinical scales usually measure the overall performance of relatively long-term medication but not short-term results, and thus $HAMD_{17}$ is not sensitive enough to detect short-term antidepressant efficacy and distinguish responders from non-responders. In this case, at the beginning of treatment, $HAMD_{17}$ scores are not predictive at the individual patient level.

Considering that the human brain functions as a large-scale complex network whose information is transmitted and integrated within spatially distributed but functionally coupled regions [56], [57], potential differences in related brain networks of these responding and non-responding patients with MDD were quantitatively analyzed to objectively evaluate the therapeutic response. First, when identifying the network changes after antidepressant treatment for one week, Fig. 3 shows the significant ($p < 0.05$) network differences in responders between 0 W and 1 W. Specifically, those patients who responded at 1 W experienced relatively decreased long-range functional connectivity between the frontal and occipital lobes (Fig. 3(a)), as well as smaller properties (Fig. 3(b)) than their 0 W measures. As reported in previous studies, abnormal activation or overloaded communication among the frontal, temporal, and occipital lobes usually occurs during the emotional and cognitive processing of patients with MDD [58], [59]. For example, Leuchter and colleagues examined coherence in the resting state and found that patients with MDD displayed higher theta and alpha coherence primarily in longer distance connections within and between electrodes overlying frontal and parieto-occipital regions [60]. Their study revealed that the strong connectivity in brain networks might be linked to impaired cognitive processing in individuals with MDD [61], including attention and working memory, as well as the processing of auditory, linguistic, and social cognition information in individuals with a psychiatric illnesses [62]. In detail, the ability to modulate alpha activity was associated with the capacity to meet working memory and executive demands and focus attention [63], [64], [65]. The increased beta activity was related to a deterioration in cognitive flexibility and control [66]. Therefore, the decreased network patterns and network properties in Fig. 3 consistently indicated that one week of medication alleviated the abnormal synchronization among those regions in patients with MDD, ameliorating related impairments in cognitive function.

Moreover, resting-state brain activity has been proven to comprise the basis of the related cognitive process [67], [68], and many studies have performed related resting-state analyses when investigating MDD dysfunction [69], [70]. In fact, the increased resting-state multiregional synchronization in patients with MDD has been proven to be accompanied by increased self-rumination, which is considered a principal cause of the psychophysiology of depression [71], [72]. Antidepressant medicines are commonly utilized to enhance monoaminergic neurotransmission and reverse some of these stress-induced neurophysiological changes, further inhibiting the abnormal activity of the amygdala, and are thus proposed to be helpful for MDD therapy [73], [74]. Here, the decreased network topologies and properties consistently clarified that one week of medication worked for responders by significantly alleviating their overall connectivity. Unfortunately, although receiving the same therapeutic intervention, the networks of those non-responding patients with MDD remained in their initial state, as no significant differences were observed between the 0 W and 1 W sessions. Here, the statistics relying on the linear mixed model did report both main effects of Group and Group-x-Time interactions for the explorations into the brain networks. The decreased network parameters consistently clarified that one week of medication worked for responders by significantly alleviating their overall connectivity. Unfortunately, although receiving the same therapeutic intervention, the networks of those non-responding patients with MDD remained in their initial state, as no significant differences were observed between the 0 W and 1 W sessions. And considering these findings, we thus assumed that the network investigation performed in our present study might be sensitive to capture the corresponding brain fluctuations occurring after one week of medication.

As resting-state networks were validated to quantitatively measure brain fluctuations after short-term treatment in patients with MDD, even within one week, the corresponding network metrics (e.g., network properties) were thus postulated to be robust biomarkers to predict therapeutic efficacy in these patients. Changes in both C and L (Fig. 4) were significantly correlated with fluctuations in $HAMD_{17}$ scores between baseline and one week of medication therapy, which primarily illustrated the possibility of the subsequent prediction analysis. Accordingly, the network properties were then utilized to predict the long-term treatment outcome. Concretely, the changes in network properties calculated by subtracting the network properties at 1 W (after one week of medication) from those at 0 W (baseline) were selected as the predictors of the eight-week antidepressant treatment response. Fig. 5 shows the scatterplots of the actual and predicted changes in the $HAMD_{17}$ scores for all of these patients with MDD, where the dashed diagonal line indicates the ideal prediction, and the blue filled circles distributed along the dashed line denote that the regression model estimated from the training set was capable of accurately predicting an individual's eight-week antidepressant outcome. In addition, considering the close correlation between network property changes and $HAMD_{17}$ score fluctuations identified in the previous analysis, this robust prediction of antidepressant outcome further validated that the network properties (C and L) indeed served as influential features to predict individual long-term medication

efficacy and verified the reliability of resting-state networks in promoting personalized medication strategies.

Due to the significant difference between 0 W and 1 W observed in responders, whereas no difference was observed in non-responders between these two stages, we further compared and analyzed the significant differences between responders and non-responders at baseline and after one week of medication. Further analysis of the data from our current study revealed that brain networks illustrated the difference between both groups, even before antidepressant treatment. Additionally, this difference between the two groups increased significantly after one week of the therapeutic intervention. Concerning the pretreatment comparison, as displayed in the left panel of Fig. 6(a), non-responders showed enhanced network connectivity compared to responders, as mainly manifested as long-range connectivity between the temporal lobe and occipital lobe. Corresponding network properties further quantitatively revealed stronger brain activity in non-responders than in responders. As validated in previous studies [75], [76], [77], [78], non-responders experienced greater abnormal activation or overloaded communication than responders, especially within the alpha band, which might result in increased functional connectivity within the default mode network of non-responders and indeed coincided with the patterns of topological differences between responders and non-responders in Fig. 6(a). Those non-responders also received one week of antidepressant medication but failed to respond. Consequently, when further investigating the potential differences between responders and non-responders after one week of medication, increasing topological differences (i.e., much stronger and denser linkages in non-responders than responders) were observed (Fig. 6(b)), which further validated the brain fluctuations given by antidepressant treatment in responding patients with MDD by inhibiting the interaction between the frontal and temporal-occipital lobes [79]. Moreover, the difference in network properties between responders and non-responders also increased substantially after one week of medication. As observed in the two histograms, the network efficiency of non-responders remained at their initial state, while a significantly smaller C and longer L of responders are illustrated in the right panel of Fig. 6, indicating treatment response.

In this regard, both resting-state network properties and topologies would help distinguish responders from non-responders. Unfortunately, when both types of information were separately applied in the present classification protocols, varying performances were achieved. Although the network properties were indeed different between these responders and non-responders, both C and L were direct statistical measurements and failed to capture the differences in network topological distributions between both groups. Therefore, a relatively low accuracy of 76.67% was achieved when the network properties were used as the discriminative features to distinguish patients with MDD in both groups. In contrast, SPN was technically developed in our previous studies [41], which mainly focused on the network topologies. More specifically, within the brain networks investigated here, the SPN adopts varied strategies for important and less important network nodes by emphasizing those important nodes with larger coefficients but suppressing others with much smaller coefficients (close to zero). As displayed in Fig. 7, those occipital electrodes (e.g., O1, O2, and Oz) are shown in a deep red or blue color and implied that great differences occurred at these electrodes, which indeed coincided with the topological differences shown in Fig. 6(a). In fact, based on these varying strategies, the SPN succeeds in extracting the network spatial information exactly and guarantees its capacity in classifying patients with MDD. Here, satisfactory performance was achieved, as the accuracy was further improved to 96.67% when using these SPN features as discriminative features. Notably, this classification is based on the EEGs recorded before the actual treatment, and it is very helpful to instruct the clinician in designing a more efficient therapeutic protocol for patients with MDD. Further, to evaluate the generalizability of our method, a total of 80 participants from four different sites were picked and then included in the categorization analysis. The recognition of responders from non-responders also obtained acceptable performance, as the accuracy of 77.50% was achieved when using SPN features as the discriminative features. Additionally, based on these merged participants, we further used related network metrics to predict the efficacy after eight-week medication; the predicted $HAMD_{17}$ changes were indeed correlated with diagnosed ones ($r = 0.50$, $p = 0.001$, $RMSE = 6.31$). These results further validated the generalizability of our proposed method in treatment selection of MDD.

Considering these findings described above, the network changes were indeed observed for the responders but not for the non-responders after short-term antidepressant treatment; and the differences between the two groups became even greater after one-week medication. Replicated evidence indicated that according to the $HAMD_{17}$ scale, antidepressant efficacy was not observed obviously until at least 4 weeks of medication [80]. However, compared with the clinical scale, the brain network seems to be a more sensitive biomarker and has a great capacity for evaluating brain changes after short-term medication, as well as distinguishing responders from non-responders. Although the exact relationship between EEG metrics and clinical scales was still unveiled, related EEG metrics Li *et al.*; Zhang *et al.* have been proved to reliably index the deficits occurring in brain diseases, as well as evaluate the treatment response from patients. Following the similar protocol used previously [81], [82], in this study, we thus utilized brain networks to quantify the brain fluctuations after one-week medication for MDD patients, and further explored the relationship between EEG metrics and clinical scale, which aimed to provide potential early biomarkers for subsequent prediction analysis and treatment selection.

However, although we have verified our method on the EMBARC study and achieved good performance, the conclusions should be further verified, and the potential capacity for big data analysis should also be confirmed. Meanwhile, we will then develop related algorithms to mitigate the site effect induced by different amplifiers and/or electrode montages to improve the generalizability and robustness of our method.

V. Conclusion

Our present study investigated the differentiable resting-state networks in both responders and non-responders between 0 W and 1 W, revealing brain fluctuations after medication in patients with MDD. Although $HAMD_{17}$ scores failed to evaluate the efficacy within the one week of medication therapy, the resting-state network properties succeeded and predicted the eight-week antidepressant treatment response at the individual patient level. Moreover, the baseline network topologies also distinguished medication responders from non-responders with an accuracy of 96.67%. Taken together, these findings consistently suggested that the brain network emerges as a sensitive biomarker to determine short-term treatment response and distinguish responders from non-responders, which provides a new bridge for adjusting the clinical treatment strategy.

References

[1] Y. Zhang *et al.*, "Identification of psychiatric disorder subtypes from functional connectivity patterns in resting-state electroencephalography," *Nature Biomed. Eng.*, vol. 5, no. 4, pp. 309–323, 2020.

[2] F. S. de Aguiar Neto and J. L. G. Rosa, "Depression biomarkers using non-invasive EEG: A review," *Neurosci. Biobehav. Rev.*, vol. 105, pp. 83–93, Oct. 2019.

[3] P. Thaipisuttikul, P. Ittasakul, P. Waleeprakhon, P. Wisajun, and S. Jullagate, "Psychiatric comorbidities in patients with major depressive disorder," *Neuropsychiatric Disease Treatment*, vol. 10, pp. 2097–2103, Jan. 2014, doi: 10.2147/ndt.S72026.

[4] A. Steffen, J. Nübel, F. Jacobi, J. Bätzing, and J. Holstiege, "Mental and somatic comorbidity of depression: A comprehensive cross-sectional analysis of 202 diagnosis groups using German nationwide ambulatory claims data," *BMC Psychiatry*, vol. 20, no. 1, p. 142, Dec. 2020, doi: 10.1186/s12888-020-02546-8.

[5] P. Blier, "Crosstalk between the norepinephrine and serotonin systems and its role in the antidepressant response," *J. Psychiatry Neurosci., JPN*, vol. 26, p. S3, Jun. 2001.

[6] M. Hamilton, "The Hamilton rating scale for depression," in *Assessment of Depression*. Nashville, TN, USA: Springer, 1986, ch. 14, pp. 143–152.

[7] N. Kappelmann *et al.*, "Psychotherapy or medication for depression? Using individual symptom meta-analyses to derive a symptom-oriented therapy (SOrT) metric for a personalised psychiatry," *BMC Med.*, vol. 18, no. 1, pp. 1–18, 2020.

[8] P. Cuijpers, C. F. Reynolds, T. Donker, J. Li, G. Andersson, and A. Beekman, "Personalized treatment of adult depression: Medication, psychotherapy, or both? A systematic review," *Depression Anxiety*, vol. 29, no. 10, pp. 855–864, Oct. 2012, doi: 10.1002/da.21985.

[9] A. Darby-Stewart and M. A. Graber, "Antidepressants for initial treatment of depression," *Amer. Family Physician*, vol. 81, no. 10, p. 1205, 2010.

[10] G. Gartlehner *et al.*, "Comparative benefits and harms of second-generation antidepressants: Background paper for the American College of Physicians," *Ann. Internal Med.*, vol. 149, no. 10, pp. 734–750, Nov. 2008, doi: 10.7326/0003-4819-149-10-200811180-00008.

[11] G. Simon, "Choosing a first-line antidepressant: Equal on average does not mean equal for everyone," Jama, vol. 286, no. 23, pp. 3003–3004, Dec. 2001, doi: 10.1001/jama.286.23.3003.

[12] A. J. Rush *et al.*, "Bupropion-SR, sertraline, or venlafaxine-XR after failure of SSRIs for depression," *New England J. Med.*, vol. 354, no. 12, pp. 1231–1242, Mar. 23 2006, doi: 10.1056/NEJMoa052963.

[13] G. E. Simon, M. Von Korff, C. M. Rutter, and D. A. Peterson, "Treatment process and outcomes for managed care patients receiving new antidepressant prescriptions from psychiatrists and primary care physicians," *Arch. Gen. Psychiatry*, vol. 58, no. 4, pp. 395–401, Apr. 2001, doi: 10.1001/archpsyc.58.4.395.

[14] E. Richelson, "Pharmacology of antidepressants," *Mayo Clinic Proc.*, vol. 76, no. 5, pp. 511–527, 2001.

[15] G. E. Simon and R. H. Perlis, "Personalized medicine for depression: Can we match patients with treatments?" *Amer. J. Psychiatry*, vol. 167, no. 12, pp. 1445–1455, 2010, doi: 10.1176/appi.ajp.2010.09111680.

[16] W. Wu *et al.*, "An electroencephalographic signature predicts antidepressant response in major depression," *Nature Biotechnol.*, vol. 38, no. 4, pp. 439–447, 2020.

[17] M. A. Martens, N. Filippini, C. J. Harmer, and B. R. Godlewska, "Resting state functional connectivity patterns as biomarkers of treatment response to escitalopram in patients with major depressive disorder," *Psychopharmacology*, pp. 1–14, 2021.

[18] J. Cui *et al.*, "Effects of escitalopram therapy on resting-state functional connectivity of subsystems of the default mode network in unmedicated patients with major depressive disorder," *Transl. Psychiatry*, vol. 11, no. 1, p. 634, 2021.

[19] R. P. Rao, *Brain-Computer Interfacing: An Introduction*. Cambridge, U.K.: Cambridge Univ. Press, 2013.

[20] C. Yi *et al.*, "A novel method for constructing EEG large-scale cortical dynamical functional network connectivity (dFNC): WTCS," *IEEE Trans. Cybern.*, early access, Aug. 16, 2021, doi: 10.1109/TCYB.2021.3090770.

[21] P. Li *et al.*, "EEG based emotion recognition by combining functional connectivity network and local activations," *IEEE Trans. Biomed. Eng.*, vol. 66, no. 10, pp. 2869–2881, Oct. 2019.

[22] F. Li *et al.*, "The dynamic brain networks of motor imagery: Time-varying causality analysis of scalp EEG," *Int. J. Neural Syst.*, vol. 29, no. 1, 2018, p. 1850016.

[23] D. S. Bassett and O. Sporns, "Network neuroscience," *Nature Neurosci.*, vol. 20, no. 3, pp. 353–364, Feb. 2017.

[24] F. Li *et al.*, "The time-varying networks in P300: A task-evoked EEG study," *IEEE Trans. Neural Syst. Rehabil. Eng.*, vol. 24, no. 7, pp. 725–733, Jul. 2016.

[25] M. Zhang *et al.*, "Randomized EEG functional brain networks in major depressive disorders with greater resilience and lower rich-club coefficient," *Clin. Neurophysiol.*, vol. 129, no. 4, pp. 743–758, 2018.

[26] M. Shim, C.-H. Im, Y.-W. Kim, and S.-H. Lee, "Altered cortical functional network in major depressive disorder: A resting-state electroencephalogram study," *NeuroImage: Clin.*, vol. 19, pp. 1000–1007, 2018.

[27] Y. Li *et al.*, "Beta oscillations in major depression—Signalling a new cortical circuit for central executive function," *Sci. Rep.*, vol. 7, no. 1, p. 18021, 2017.

[28] S. Mahato, N. Goyal, D. Ram, and S. Paul, "Detection of depression and scaling of severity using six channel EEG data," *J. Med. Syst.*, vol. 44, no. 7, p. 118, Jul. 2020, doi: 10.1007/s10916-020-01573-y.

[29] H. Cai, X. Sha, X. Han, S. Wei, and B. Hu, "Pervasive EEG diagnosis of depression using deep belief network with three-electrodes EEG collector," in *Proc. IEEE Int. Conf. Bioinf. Biomed. (BIBM)*, Dec. 2016, pp. 1239–1246.

[30] Y. Mohammadi and M. H. Moradi, "Prediction of depression severity scores based on functional connectivity and complexity of the EEG signal," *Clin. EEG Neurosci.*, vol. 52, no. 1, pp. 52–60, Jan. 2021.

[31] X. Li, Z. Jing, B. Hu, and S. Sun, "An EEG-based study on coherence and brain networks in mild depression cognitive process," in *Proc. IEEE Int. Conf. Bioinf. Biomed. (BIBM)*, Dec. 2016, pp. 1275–1282.

[32] M. Yu *et al.*, "Childhood trauma history is linked to abnormal brain connectivity in major depression," *Proc. Nat. Acad. Sci. USA*, vol. 116, no. 17, pp. 8582–8590, Apr. 2019.

[33] M. H. Trivedi *et al.*, "Establishing moderators and biosignatures of antidepressant response in clinical care (EMBARC): Rationale and design," *J. Psychiatric Res.*, vol. 78, pp. 11–23, Jul. 2016.

[34] D.-J. Kim *et al.*, "Disturbed resting state EEG synchronization in bipolar disorder: A graph-theoretic analysis," *NeuroImage, Clin.*, vol. 2, pp. 414–423, Mar. 2013.

[35] M. Rubinov and O. Sporns, "Complex network measures of brain connectivity: Uses and interpretations," *NeuroImage*, vol. 52, no. 3, pp. 1059–1069, Apr. 2010.

[36] V. Sakkalis, "Review of advanced techniques for the estimation of brain connectivity measured with EEG/MEG," *Comput. Biol. Med.*, vol. 41, no. 12, pp. 1110–1117, 2011.

[37] J. Sun, Z. Li, and S. Tong, "Inferring functional neural connectivity with phase synchronization analysis: A review of methodology," *Comput. Math. Methods Med.*, vol. 2012, Apr. 2012, Art. no. 239210.

[38] P. Celka, "Statistical analysis of the phase-locking value," *IEEE Signal Process. Lett.*, vol. 14, no. 9, pp. 577–580, Sep. 2007.

[39] Y. Dasdemir, E. Yildirim, and S. Yildirim, "Analysis of functional brain connections for positive–negative emotions using phase locking value," *Cogn. Neurodyn.*, vol. 11, no. 6, pp. 487–500, 2017.

[40] T. Zhang *et al.*, "Structural and functional correlates of motor imagery BCI performance: Insights from the patterns of fronto-parietal attention network," *NeuroImage*, vol. 134, pp. 475–485, Jul. 2016, doi: 10.1016/j.neuroimage.2016.04.030.

[41] F. Li *et al.*, "Differentiation of schizophrenia by combining the spatial EEG brain network patterns of rest and task P300," *IEEE Trans. Neural Syst. Rehabil. Eng.*, vol. 27, no. 4, pp. 594–602, Apr. 2019.

[42] P. Xu *et al.*, "Differentiating between psychogenic nonepileptic seizures and epilepsy based on common spatial pattern of weighted EEG resting networks," *IEEE Trans. Biomed. Eng.*, vol. 61, no. 6, pp. 1747–1755, Jun. 2014.

[43] K. Duan *et al.*, "Discrimination of Tourette syndrome based on the spatial patterns of the resting-state EEG network," *Brain Topography*, vol. 34, no. 1, pp. 78–87, 2021.

[44] Y. Si *et al.*, "Predicting individual decision-making responses based on single-trial EEG," *NeuroImage*, vol. 206, Feb. 2020, Art. no. 116333.

[45] P. Xu, M. Kasprowicz, M. Bergsneider, and X. Hu, "Improved non-invasive intracranial pressure assessment with nonlinear kernel regression," *IEEE Trans. Inf. Technol. Biomed.*, vol. 14, no. 4, pp. 971–978, Jul. 2010.

[46] L.-L. Zeng *et al.*, "Identifying major depression using whole-brain functional connectivity: A multivariate pattern analysis," *Brain*, vol. 135, no. 5, pp. 1498–1507, 2012.

[47] A. Yasuhara, "Correlation between EEG abnormalities and symptoms of autism spectrum disorder (ASD)," *Brain Develop.*, vol. 32, no. 10, pp. 791–798, 2010.

[48] Y. Mohan, S. Seng Chee, D. Kan Pei Xin, and L. Poh Foong, "Artificial neural network for classification of depressive and normal in EEG," in *Proc. IEEE EMBS Conf. Biomed. Eng. Sci. (IECBES)*, Dec. 2016, pp. 286–290.

[49] W. J. Bosl, H. Tager-Flusberg, and C. A. Nelson, "EEG analytics for early detection of autism spectrum disorder: A data-driven approach," *Sci. Rep.*, vol. 8, no. 1, p. 6828, 2018.

[50] D. P. X. Kan and P. F. Lee, "Decrease alpha waves in depression: An electroencephalogram (EEG) study," in *Proc. Int. Conf. BioSignal Anal., Process. Syst. (ICBAPS)*, May 2015, pp. 156–161.

[51] J. Busner and S. D. Targum, "The clinical global impressions scale: Applying a research tool in clinical practice," *Psychiatry (Edgmont)*, vol. 4, no. 7, p. 28, 2007.

[52] F. N. Jacka *et al.*, "A randomised controlled trial of dietary improvement for adults with major depression (the 'SMILES' trial)," *BMC Med.*, vol. 15, no. 1, pp. 1–13, 2017.

[53] E. Maris and R. Oostenveld, "Nonparametric statistical testing of EEG- and MEG-data," *J. Neurosci. Methods*, vol. 164, no. 1, pp. 177–190, 2007.

[54] R. M. Bagby, A. G. Ryder, D. R. Schuller, and M. B. Marshall, "The Hamilton depression rating scale: Has the gold standard become a lead weight?" *Amer. J. Psychiatry*, vol. 161, no. 12, pp. 2163–2177, 2004, doi: 10.1176/appi.ajp.161.12.2163.

[55] R. Machado-Vieira *et al.*, "The timing of antidepressant effects: A comparison of diverse pharmacological and somatic treatments," *Pharmaceuticals*, vol. 3, no. 1, pp. 19–41, 2010.

[56] Q. K. Telesford, S. L. Simpson, J. H. Burdette, S. Hayasaka, and P. J. Laurienti, "The brain as a complex system: Using network science as a tool for understanding the brain," *Brain Connectivity*, vol. 1, no. 4, pp. 295–308, 2011.

[57] D. B. Dwyer *et al.*, "Large-scale brain network dynamics supporting adolescent cognitive control," *J. Neurosci.*, vol. 34, no. 42, pp. 14096–14107, 2014.

[58] V. S. Rotenberg, "The peculiarity of the right-hemisphere function in depression: Solving the paradoxes," *Prog. Neuro-Psychopharmacol. Biol. Psychiatry*, vol. 28, no. 1, pp. 1–13, 2004.

[59] A. F. Leuchter, I. A. Cook, A. M. Hunter, C. Cai, and S. Horvath, "Resting-state quantitative electroencephalography reveals increased neurophysiologic connectivity in depression," *PLoS ONE*, vol. 7, no. 2, Feb. 2012, Art. no. e32508.

[60] A. F. Leuchter, I. A. Cook, A. M. Hunter, C. Cai, and S. Horvath, "Resting-state quantitative electroencephalography reveals increased neurophysiologic connectivity in depression," *PLoS ONE*, vol. 7, no. 2, 2012, Art. no. e32508.

[61] M. D. Greicius *et al.*, "Resting-state functional connectivity in major depression: Abnormally increased contributions from subgenual cingulate cortex and thalamus," *Biol. Psychiatry*, vol. 62, no. 5, pp. 429–437, 2007.

[62] M. K. Fulton, R. Armitage, and A. J. Rush, "Sleep electroencephalographic coherence abnormalities in individuals at high risk for depression: A pilot study," *Biol. Psychiatry*, vol. 47, no. 7, pp. 618–625, Apr. 2000.

[63] C. Del Percio *et al.*, "Functional coupling of parietal alpha rhythms is enhanced in athletes before visuomotor performance: A coherence electroencephalographic study," *Neuroscience*, vol. 175, pp. 198–211, Feb. 2011.

[64] C. Babiloni, A. Brancucci, F. Vecchio, L. Arendt-Nielsen, A. C. N. Chen, and P. M. Rossini, "Anticipation of somatosensory and motor events increases centro-parietal functional coupling: An EEG coherence study," *Clin. Neurophysiol.*, vol. 117, no. 5, pp. 1000–1008, 2006.

[65] P. J. Uhlhaas and W. Singer, "Neural synchrony in brain disorders: Relevance for cognitive dysfunctions and pathophysiology," *Neuron*, vol. 52, no. 1, pp. 155–168, Oct. 2006.

[66] A. K. Engel and P. Fries, "Beta-band oscillations—Signalling the status quo?" *Current Opinion Neurobiol.*, vol. 20, no. 2, pp. 156–165, 2010.

[67] O. Y. Chén *et al.*, "Resting-state brain information flow predicts cognitive flexibility in humans," *Sci. Rep.*, vol. 9, no. 1, p. 3879, 2019.

[68] R. Zhang *et al.*, "Efficient resting-state EEG network facilitates motor imagery performance," *J. Neural Eng.*, vol. 12, no. 6, Dec. 2015, Art. no. 066024.

[69] A. A. Fingelkurts and A. A. Fingelkurts, "Altered structure of dynamic electroencephalogram oscillatory pattern in major depression," *Biol. Psychiatry*, vol. 77, no. 12, pp. 1050–1060, 2015.

[70] J.-S. Lee, B.-H. Yang, J.-H. Lee, J.-H. Choi, I.-G. Choi, and S.-B. Kim, "Detrended fluctuation analysis of resting EEG in depressed outpatients and healthy controls," *Clin. Neurophysiol.*, vol. 118, no. 11, pp. 2489–2496, 2007.

[71] J. Joireman, "Empathy and the self-absorption paradox II: Self-rumination and self-reflection as mediators between shame, guilt, and empathy," *Self Identity*, vol. 3, no. 3, pp. 225–238, 2004.

[72] F. Sambataro, N. D. Wolf, M. Pennuto, N. Vasic, and R. C. Wolf, "Revisiting default mode network function in major depression: Evidence for disrupted subsystem connectivity," *Psychol. Med.*, vol. 44, no. 10, pp. 2041–2051, Jul. 2014.

[73] G. Serafini, "Neuroplasticity and major depression, the role of modern antidepressant drugs," *World J. Psychiatry*, vol. 2, no. 3, p. 49, 2012.

[74] C. Andrade and N. K. Rao, "How antidepressant drugs act: A primer on neuroplasticity as the eventual mediator of antidepressant efficacy," *Indian J. Psychiatry*, vol. 52, no. 4, p. 378, 2010.

[75] V. J. Knott, J. I. Telner, Y. D. Lapierre, M. Browne, and E. R. Horn, "Quantitative EEG in the prediction of antidepressant response to imipramine," *J. Affect. Disorders*, vol. 39, no. 3, pp. 175–184, 1996.

[76] D. V. Iosifescu, "Electroencephalography-derived biomarkers of antidepressant response," *Harvard Rev. Psychiatry*, vol. 19, no. 3, pp. 144–154, 2011.

[77] G. E. Bruder *et al.*, "Electroencephalographic and perceptual asymmetry differences between responders and nonresponders to an SSRI antidepressant," *Biol. Psychiatry*, vol. 49, no. 5, pp. 416–425, 2001.

[78] G. E. Bruder, J. P. Sedoruk, J. W. Stewart, P. J. McGrath, F. M. Quitkin, and C. E. Tenke, "Electroencephalographic alpha measures predict therapeutic response to a selective serotonin reuptake inhibitor antidepressant: Pre- and post-treatment findings," *Biol. Psychiatry*, vol. 63, no. 12, pp. 1171–1177, 2008.

[79] M. Bellani, N. Dusi, P.-H. Yeh, J. C. Soares, and P. Brambilla, "The effects of antidepressants on human brain as detected by imaging studies. Focus on major depression," *Prog. Neuro-Psychopharmacol. Biol. Psychiatry*, vol. 35, no. 7, pp. 1544–1552, 2011.

[80] P. A. Kudlow, R. S. McIntyre, and R. W. Lam, "Early switching strategies in antidepressant non-responders: Current evidence and future research directions," *CNS Drugs*, vol. 28, no. 7, pp. 601–609, 2014.

[81] E. Gaily, E. Liukkonen, R. Paetau, M. Rekola, and M. L. Granström, "Infantile spasms: Diagnosis and assessment of treatment response by video-EEG," *Developmental Med. Child Neurol.*, vol. 43, no. 10, pp. 658–667, 2001.

[82] A. D. Krystal and R. D. Weiner, "EEG correlates of the response to ECT: A possible antidepressant role of brain-derived neurotrophic factor," *J. ECT*, vol. 15, no. 1, pp. 27–38, 1999.